ADVISORY GROUP FOR AERONAUTICAL RESEARCH AND DEVELOPMENT

64 RUE DE VARENNE, PARIS VII

REPORT 323

THERMODYNAMIC AND TRANSPORT PROPERTIES OF HIGH-TEMPERATURE AIR

by

C. F. HANSEN

SEPTEMBER 1959

NORTH ATLANTIC TREATY ORGANISATION

REPORT 323

NORTH ATLANTIC TREATY ORGANIZATION

ADVISORY GROUP FOR AERONAUTICAL RESEARCH AND DEVELOPMENT

THERMODYNAMIC AND TRANSPORT PROPERTIES OF HIGH-TEMPERATURE AIR

by

C. Frederick Hansen

This Report is one in the series 320-333 of papers presented at the High Temperature Gas Characteristics Meeting of the AGARD Wind Tunnel and Model Testing Panel (now Fluid Dynamics Panel) held 21-23 September 1959, in Aachen, Germany

SUMMARY

It is well known that vehicles traveling at high speed excite the air to high temperature, resulting in dissociation and ionization, so that the air properties deviate considerably from those of a simple gas. Some effects of these reactions are considered in this Report in relation to the thermodynamic properties of the air, the transport coefficients, and the diffusion of heat.

Methods are presented for calculating the thermodynamic properties of air with good accuracy up to 15,000° K and for pressures from 10^{-6} to 10^{2} atmospheres.

SOMMAIRE

Ainsi qu'il est bien connu, le vol à grande vitesse de tout engin provoque des températures élevées de l'air, donnant lieu en conséquence aux phénomènes de la dissociation et de l'ionisation, de sorte que les caractéristiques de l'air diffèrent sensiblement de celles d'un gaz simple. Il s'agit dans ce rapport de certains effets résultant de ces réactions considérés en fonction des propriétés thermodynamiques de l'air, des coefficients de transport et de la diffusion de chaleur.

L'auteur présente des procédés de calcul des caractéristiques thermodynamiques de l'air, avec une bonne précision pour des températures s'élevant à 15.000°K et des pressions comprises entre 10^{-6} et 10^{2} atm.

536.7

1c3b:3b1e

CONTENTS

LIST OF FIGURES

NOTATION

R	universal gas constant
p	pressure
ρ	density
T	temperature
M_0	molecular weight at standard conditions
Z	total number of moles from one mol of initially undissociated air
ϵ_1	fraction of oxygen molecules dissociated
ϵ_2	fraction of nitrogen molecules dissociated
ϵ_3	fraction of atoms ionized
K_1	equilibrium constant for reaction $O_2 \rightarrow 2O$
K_2	equilibrium constant for reaction $N_2 \rightarrow 2N$
K_3	population - weighted average of equilibrium constants for reactions $O \rightarrow O^+ + e^-$ and $N \rightarrow N^+ + e^-$
x_i	mol fraction of chemical species
H	enthalpy per mol
S	entropy per mol
Q_i	partition function for i^{th} species
γ	ratio of specific heats
c	speed of sound
v	velocity of flow
v_i	velocity of flow at initial conditions
x	distance
t	time
r	distance between atoms
σ	collision diameter

σ'	mass diffusion diameter
r_e	constants
β	constants
D	constants
k	constants
e	electron charge
α	polarizability
η_e	total charge density
μ	viscosity
u_i	mean molecular velocity of i^{th} species
λ_i	mean free path of i^{th} species
n	particle concentration
κ	partial coefficient of thermal conductivity
ϕ	heat flux potential
α	thermal diffusivity $(= k/\rho C_p)$
C	coefficient of heat capacity
Pr	Prandtl number

THERMODYNAMIC AND TRANSPORT PROPERTIES OF HIGH-TEMPERATURE AIR

C. Frederick Hansen*

1. INTRODUCTION

It is axiomatic that the science of aerodynamics must be based on a good understanding of the medium through which vehicles fly. At subsonic and low supersonic speeds near the earth's surface, it is generally sufficient to assume that the atmosphere behaves as an ideal gas and that the ratio of specific heats is a constant with a value about 1.4. However, it is well known that vehicles traveling at high speed excite the air to high temperature with the result that air properties deviate considerably from those of a simple gas. For example, Figure 1 shows the major chemical reactions which are produced in the stagnation regions of vehicles as a function of altitude and velocity. At about 3000 ft/sec, the vibrational energy of air molecules is excited. Oxygen dissociation begins near 7000 ft/sec and nitrogen dissociation occurs at velocities greater than 15,000 ft/sec. Single ionization of atoms becomes dominant near escape velocity. The dissociation reactions are encouraged by low pressure, of course, and the altitude dependence shown in Figure 1 is a consequence of this fact. Some effects of these chemical reactions will be considered pertaining to the thermodynamic properties of air, to some of the transport coefficients, and to the diffusion of heat through gases.

2. EQUILIBRIUM THERMODYNAMIC PROPERTIES OF AIR

The equilibrium thermodynamic properties of gases can be calculated with good confidence, provided the energy levels of the gas particles are accurately known, and a number of such calculations have been tabulated for air. Perhaps the most complete and exacting calculations are those performed by Gilmore[1] and by Hilsenrath and Beckett[2]. Both of these calculations are very exact in the sense that they take into account many of the minor chemical components of air and small corrections to the partition functions of the molecules. Logan and Treanor[3] have also prepared tables of air properties for which all of the important components are considered. These precise calculations involve multiple iteration procedures such that the labor involved would be discouraging indeed, if it were not for electronic computers.

The content of the tabulations in References 2 and 3 has been summed up graphically in the Mollier diagrams prepared by Feldman[4] and by Moeckel[5]. Using such graphs one can solve a number of important aerodynamic problems, such as finding the properties of isentropic expansions or of non-isentropic shock discontinuities (see, e.g., Ref. 4, 6, 7, or 8).

For a number of reasons, it is desirable to have approximate, analytic solutions for the thermodynamic properties of air in addition to the precise solutions mentioned

---

*Chief, Physics Branch, National Aeronautics and Space Administration, Ames Research Center, Moffett Field, California, U.S.A.

above. From an inspection of the tabulated equilibrium concentrations of the chemical species in air[1], it is immediately apparent that there are but four reactions of major importance over a wide range of pressure and temperature. These are the dissociation of molecular oxygen and of molecular nitrogen, and the ionization of atomic oxygen and atomic nitrogen:-

$$O_2 \rightarrow 2O \tag{1}$$

$$N_2 \rightarrow 2N \tag{2}$$

$$O \rightarrow O^+ + e^- \tag{3}$$

$$N \rightarrow N^+ + e^- \tag{4}$$

With one exception, all other reactions yield concentrations which are of the order of 0.1%, or less, of the major components given by these reactions. The exception is the formation of nitric oxide, which may become a sizable minor component of air at high pressures (see Ref. 1). However, the heat of formation of NO is very nearly the average of that for O_2 and N_2, so the production of NO does not appreciably change the balance between atoms and molecules. As a result, the thermodynamic functions for air are not strongly influenced by this reaction.

Some distinctive features of the foregoing reactions are conveniently summarized on a graph of the compressibility as a function of temperature (Fig. 2). The compressibility is defined by the gas law

$$\frac{p}{\rho} = Z\left(\frac{RT}{M_0}\right) \tag{5}$$

where R is the universal gas constant, p, ρ and T are, respectively, the pressure, density and temperature of the gas, and M_0 is the molecular weight at standard conditions. To the approximation that the particles obey the ideal gas law, Z represents the total number of moles formed from a mol of initially undissociated air. Since air contains about 20% oxygen, the compressibility approaches 1.2 when oxygen dissociation is complete. It increases further to about 2.0 when nitrogen dissociation finishes the conversion of molecules into atoms. Single ionization of the atoms doubles the number of gas particles again, so that Z approaches 4.0 when these reactions are complete. Note that the slope of Z gets very small between reactions, indicating that one reaction is essentially complete before the next begins. This follows from the fact that the dissociation energy of nitrogen (9.76 ev) is nearly twice the dissociation energy of oxygen (5.08 ev), while the ionization energy of nitrogen atoms (14.54 ev) and oxygen atoms (13.61 ev) is nearly three times as great. Thus the different reactions proceed in different intervals of temperature, and for purposes of approximation it can be assumed that they are independent of one another. The two ionization reactions occur simultaneously but with nearly the same energy changes, so for this case it is assumed that, once the air becomes dissociated, all atoms constitute a single species which has the population-weighted average properties of the nitrogen and oxygen atoms.

We shall review briefly some of the essential relations involved in calculating the approximate thermodynamic properties of air. Further details may be found in

Reference 9. If ϵ_1 is the fraction of oxygen molecules which are dissociated, ϵ_2 the fraction of nitrogen molecules dissociated, and ϵ_3 the fraction of atoms which are ionized, then the compressibility is

$$Z = 1 + \epsilon_1 + \epsilon_2 + 2\epsilon_3 \tag{6}$$

The reactions are assumed to be completely independent and, to the order of approximation being considered, it seems adequate to take the ratio of nitrogen to oxygen in air as 4 to 1. Then one obtains

$$\epsilon_1 = \frac{-0.8 + \sqrt{0.64 + 0.8\left(1 + \frac{4p}{K_1}\right)}}{2\left(1 + \frac{4p}{K_1}\right)} \tag{7a}$$

$$\epsilon_2 = \frac{-0.4 + \sqrt{0.16 + 3.84\left(1 + \frac{4p}{K_2}\right)}}{2\left(1 + \frac{4p}{K_2}\right)} \tag{7b}$$

$$\epsilon_3 = \frac{1}{\sqrt{(1 + p/K_3)}} \tag{7c}$$

where K_1 and K_2 are, respectively, the equilibrium constants for reactions (1) and (2) in terms of partial pressures; K_3 is the population-weighted average of the equilibrium constants for reactions (3) and (4). The equilibrium constants are calculated from partition functions which include only those energy levels up to 6 kT (8.76 ev at 15,000°K). The energy, entropy and specific heats of the components are also calculated from these abbreviated partition functions.

The form of Equations (7a) through (7c) is suitable for constant pressure calculations. For constant density calculations, these equations become

$$\epsilon_1 = \frac{-1 + \sqrt{1 + \frac{3.2\rho RT}{K_1 M_0}}}{\frac{8\rho RT}{K_1 M_0}} \tag{8a}$$

$$\epsilon_2 = \frac{-1 + \sqrt{1 + \frac{12.8\rho RT}{K_2 M_0}}}{\frac{8\rho RT}{K_2 M_0}} \tag{8b}$$

$$\epsilon_3 = \frac{-1 + \sqrt{1 + \dfrac{8\rho RT}{K_3 M_0}}}{\dfrac{4\rho RT}{K_3 M_0}} \tag{8c}$$

At this point it may be remarked that the formation of NO can be included in the closed form approximations if one is willing to go to the trouble of solving cubic equations rather than the foregoing quadratic expressions.

The mol fractions x_i of the chemical species are given by

$$x_{O_2} = \frac{0.2 - \epsilon_1}{Z} \tag{9a}$$

$$x_{N_2} = \frac{0.8 - \epsilon_2}{Z} \tag{9b}$$

$$x_O = \frac{2\epsilon_1 - 0.4\epsilon_3}{Z} \tag{9c}$$

$$x_N = \frac{2\epsilon_2 - 1.6\epsilon_3}{Z} \tag{9d}$$

$$x_{N^+ + O^+} = x_{e^-} = \frac{2\epsilon_3}{Z} \tag{9e}$$

and the enthalpy and entropy for the mixture are found by a simple summation over all the species

$$\frac{H}{RT} = \sum_i x_i \frac{d(ln\ Q_i)}{d(ln\ T)} \tag{10}$$

$$\frac{S}{R} = \sum_i \left[x_i \left(ln\ Q_i + \frac{d(ln\ Q_i)}{d(ln\ T)} \right) - x_i (ln\ x_i) \right] - ln \frac{p}{p_0} \tag{11}$$

The symbols H and S refer to the enthalpy and entropy per mol of particles and Q_i is the partition function for the i^{th} species at the standard state pressure p_0. Note that the N^+ and O^+ fractions should be considered separately for the term $x_i(ln\ x_i)$ which appear in the entropy (Eq. 11), though they may be combined elsewhere.

The accuracy of the foregoing approximations is indicated in Figures 3(a) through 3(d). Figure 3(a) shows the percentage discrepancy between the compressibility given by Equation (6) and the solutions of Hilsenrath and Beckett[2] for densities of 10^2, 10^{-2} and 10^{-6} Amagat. Figures 3(b) and 3(c) show the same comparison for enthalpy and entropy.

It can be seen that the discrepancies are generally less than 5%, sufficient for many engineering purposes. The largest discrepancies occur at high densities where there is some overlapping of the reactions and where the formation of nitric oxide should be taken into account for greater accuracy.

The specific heats of air may be found by taking the derivatives of energy and enthalpy. The approximations lose accuracy with each successive order derivative, of course, but still the agreement is generally within 10% of the iteration solutions performed by Logan[3]. Fortunately, one does not usually use the specific heats directly in aerodynamic calculations anyway, but rather the ratio of specific heats, γ. As shown in Figure 3(d), the approximations preserve the accuracy of this quantity within a few percent.

The speed of sound, c, will be defined by

$$c^2 = \left(\frac{\partial p}{\partial \rho}\right)_s \tag{12}$$

which may be transformed to

$$\frac{c^2 \rho}{p} = \gamma \frac{1 + \left(\frac{\partial (ln\ Z)}{\partial (ln\ T)}\right)_\rho}{1 + \left(\frac{\partial (ln\ Z)}{\partial (ln\ T)}\right)_p} \tag{13}$$

Using this quantity, one can evaluate the integral

$$l = \int_0^p \frac{dp}{c\rho} \tag{14}$$

which is useful for determining the Riemann invariants $v \pm l$ for one-dimensional, isentropic flow. The change in velocity along the characteristic directions in such gas flow is given[10] by

$$v - v_i = \pm (l_i - l) \tag{15}$$

where the subscript i refers to initial conditions and the positive sign corresponds to the positive characteristic direction

$$\frac{dx}{dt} = v + c \tag{16a}$$

and the negative sign to the negative characteristic direction

$$\frac{dx}{dt} = v - c \tag{16b}$$

in the time-distance (x,t) plane. The integration of Equation (14) is along a constant isentrope, and the solutions are performed by iteration with an electronic computer inasmuch as entropy is not one of the independent variables in the analytic expressions for the gas properties. Where very small changes in flow properties are desired, as in the construction of a fine net characteristics solution, it is more convenient to work with just the integrand of Equation (14). Small changes in flow velocity are approximately given by

$$v - v_i \simeq \left(\frac{p}{c\rho}\right)\frac{\Delta p}{p} \tag{17}$$

where the algebraic sign of the pressure change Δp corresponds to the sign of the characteristic direction. The quantity

$$I = \left(\frac{p}{c\rho}\right) \tag{18a}$$

is plotted in Figure 4 normalized by the ideal air value

$$I^* = \sqrt{\frac{RT}{\gamma}} \tag{18b}$$

where γ is taken equal to 1.4. The ratios are given as functions of temperature for isentropes ZS/R equal to 30, 40, 50, 60, 70, 80, 90 and 100. Values for intermediate entropies may be estimated reasonably well by interpolation. Numerical values of I/I^* and l are tabulated in Reference 11.

3. TRANSPORT PROPERTIES OF AIR

Next consider some additional properties of air needed for aerodynamic calculations, namely the transport properties viscosity and thermal conductivity. In estimating these properties, one is faced with two alternatives. The transport coefficients may be calculated by the fairly rigorous but complex method of Chapman and Enskog[12] or by the simple but approximate kinetic theory of hard, elastic spheres[13]. If good estimates of the interparticle potentials were available, so that the Enskog collision integrals could be determined accurately, the choice would immediately fall on the former method, of course. However, at present the potentials are uncertain enough so that it is doubtful whether the inherent accuracy of the more rigorous method could be realized. Inasmuch as encouraging progress is being made on quantum mechanical calculations of the interparticle potentials (see, e.g., Refs. 14 through 17), it has been decided to defer the labor of making the rigorous solutions until all of the important potentials are available. In the meantime, some estimates based on the simple kinetic theory have been prepared. It may be noted that this elementary approach need not be discounted unduly, for it does give reasonably good answere where experimental evidence is available for comparison.

The first step is the calculation of mean free paths from the effective collision diameters. Hirschfelder and Eliason[18] have found that for a wide variety of different attractive potentials, the collision integral method corresponds to an effective hard

sphere diameter equal to the distance where the interparticle potential is about -0.6 kT. In the case of repulsive potentials, the effective diameter for momentum and energy transport is the distance between the atoms when the potential is about 0.9 kT, while for mass diffusion it occurs at about 1.6 kT. These simple criteria might be applied if only the potentials were known. Unfortunately, in the case of atom-atom and atom-ion collisions, the picture is complicated by the fact that the particles may approach one another along any one of a number of different potentials, depending on how the electron spin vectors happen to add up. For example, Figure 5 shows the qualitative form of the potentials for collisions between two neutral, ground-state nitrogen atoms as a function of the distance r between atoms[19]. The lowest lying potential, $^1\Sigma$, has the lowest total electron spin and it is known quantitatively from the vibrational energy levels observed spectroscopically for the stable ground state molecule. Since the higher lying potentials are not known quantitatively, we are forced to estimate the average effective size from the single known potential. For this purpose, it has been assumed that the average effective collision diameter is the distance between the atoms when $U(^1\Sigma)$ equals -kT for the case of momentum and energy flux, and -2 kT for mass diffusion. This procedure undoubtedly overestimates the size of shallow intermediate potentials (such as $^3\Sigma$ and $^5\Sigma$ - Fig. 5). On the other hand it underestimates the relatively long-range forces between particles in excited states. The very steep repulsive potentials (such as $^7\Sigma$ of Fig. 5) are roughly symmetrical with the lowest attractive potential over the long-range part of the internuclear separation distance, so this potential is probably correctly accounted for to a first approximation.

To be more specific, the following formulas were used for calculating collision cross sections (a Sutherland type cross section is used for oxygen and nitrogen molecules):

$$\frac{S}{S_\infty} = 1 + \frac{C}{T} \tag{19}$$

where the constant C is 112° K and S_∞, the molecular cross section at very high temperature, is 3.14×10^{-15} cm^2. The lowest lying atom-atom and atom-ion potentials may be approximated by the Morse function

$$\frac{U}{D} = \left[1 - e^{-\beta(r/r_e - 1)}\right]^2 - 1 \tag{20}$$

whence the collision diameter for momentum and energy transfer, σ, is given by

$$\frac{\sigma}{r_e} = 1 - \frac{1}{\beta} ln \left(1 - \sqrt{1 - \frac{kT}{D}}\right) \tag{21a}$$

and the diameter for mass diffusion, σ', is

$$\frac{\sigma'}{r_e} = 1 - \frac{1}{\beta} ln \left(1 - \sqrt{1 - \frac{2kT}{D}}\right) \tag{21b}$$

The constants r_e, β, and D/k for the various types of collisions are taken from

Herzberg[19] and these are listed in the following table:

Colliding particles	D/k (^{o}K)	β	r_e *(Angstroms)*
O-O	59,000	3.24	1.207
N-N	113,200	2.96	1.094
N-O	75,400	3.18	1.151
$O\text{-}O^+$	75,200	3.18	1.123
$N\text{-}N^+$	101,200	2.94	1.116

For electron-atom collisions, the atom becomes polarized by the approach of the electron and a charge-dipole type of interaction results. The classical interaction energy of the induced dipole with the electron's field is

$$U = -\frac{e^2\alpha}{2r^4} \tag{22}$$

where e is the electron charge and α is the polarizability. The polarizability is taken to be $13.2 \times 10^{-25}cm^3$ and $10.3 \times 10^{-25}cm^3$ for oxygen and nitrogen atoms, respectively. The quantum mechanical cross sections calculated by Hammerling, Shine and Kivel[16] show that the Hartree electrostatic field and the exchange integrals both contribute to the interaction energy as well as the polarization. However, they find that these two effects roughly compensate one another, and so these corrections will be omitted for the approximation being considered here.

Finally, the ion-ion and ion-electron cross sections are calculated from the simple Coulomb potential between two charges. The correction for the charge shielding effect given by Cohen, Spitzer and Routly[20] makes the cross sections weakly dependent on density as follows:

$$S = \pi\left(\frac{e^2}{kT}\right)^2 ln\ \frac{3}{2e^3}\left(\frac{k^3T^3}{\pi n_e}\right)^{1/2} \tag{23}$$

where n_e is the total charge density, both positive and negative.

The viscosity was calculated from the simple summation formula for a mixture of hard spherical molecules[13]:

$$\mu = \frac{5\pi}{32}\sum_i \rho_i u_i \lambda_i \tag{24}$$

where u_i is the mean molecular velocity of the i^{th} species and the mean free path λ_i is given by

$$\lambda_i = \frac{1}{2n \sum_j x_j S_{ij} \left(1 + \frac{M_i}{M_j}\right)^{-1/2}} \tag{25}$$

where n is the particle concentration. Equation (25) differs from Kennard's expression for the mean free path[13] to account for the fact that the momentum of particle i relative to particle j is decreased by the fraction $2(1 + M_i/M_j)^{-1}$ on each elastic collision with particle j. This factor multiplies each term of the summation in the denominator of Kennard's formula, and the result is the same as obtained in the more rigorous matrix formulation for the viscosity of mixtures[21] if the off-diagonal elements of the matrix are set equal to zero. This is valid in a first approximation at least, as the off-diagonal elements are small compared to the trace elements of the matrix. Buddenberg and Wilke[22] have shown that experimental data on the viscosity of mixtures can be reproduced by empirically adjusting the numerical factor 2 before those terms of the summation in Equation 25 which involve unlike particles ($i \neq j$). However, in view of the other approximations involved in the present analysis, it did not seem warranted to use a more sophisticated formulation for the viscosity of the mixture than given above. The estimated viscosities are shown as a function of temperature for pressures of 10^0, 10^{-2} and 10^{-4} atmospheres in Figure 6. The ordinate is the ratio of the coefficient given by Equation (24) to the value given by the Sutherland formula:

$$\mu_0 = 1.462 \times 10^{-5} \frac{\sqrt{T}}{1 + \frac{112}{T}} \quad \frac{gm}{cm\ sec} \tag{26}$$

where T is in degrees Kelvin. Presumably, Equation (26) is about the viscosity which the gas would have if air molecules remained inert. The effect of the dissociation reactions is to increase slightly the ratio μ/μ_0. However, the charged particles have very large cross sections when they collide with one another, so the viscosity is reduced to comparatively low values at the higher temperatures where ionization becomes predominant.

A theory for the thermal conductivity of a chemically reacting gas was first outlined by Nernst[23]. The theory is used here in the form subsequently developed by Hirschfelder[24], in which the energy transfer through the gas is treated in two independent parts. The first mode of energy transfer is by molecular collisions just as for ordinary non-reactive gases. The second mode of energy transfer is by diffusion of the molecular species and the reactions which occur as the gas tends to maintain itself in chemical equilibrium. For the first mode, use is made of Eucken's assumption[25] that the internal energy is distributed among the gas particles independently of the velocity distribution, so that the partial coefficient of thermal conductivity takes the form

$$\kappa_{inert} = \frac{5\pi}{32} \sum_i \rho_i u_i \lambda_i \left(\frac{C_i}{M_i} + \frac{9}{4}\frac{R}{M_i}\right) \tag{27}$$

Hirschfelder formulates the reactive contribution to thermal conductivity in terms of the multicomponent diffusion coefficients which are somewhat difficult to estimate. However, Butler and Brokaw[26] have shown that the reactive coefficient of conductivity may be expressed in terms of the ordinary binary diffusion coefficients, D_{ij}:

$$\kappa_{reactive} = \frac{nk\left(\frac{d(ln\ K)}{d(ln\ T)}\right)^2}{\sum_i \sum_j \frac{a_i}{x_i D_{ij}} (a_i x_j - a_j x_i)} \tag{28}$$

where the a_i's are the stoichiometric coefficients of the components A_i when the chemical reaction is written in the form

$$\sum_i a_i A_i = 0 \tag{29}$$

The diffusion coefficients are calculated by elementary kinetic theory as follows[13]:

$$\frac{1}{D_{ij}} = \frac{8}{3}\left(\frac{2}{\pi RT}\frac{M_i M_j}{M_i + M_j}\right) n S_{ij} \tag{30}$$

The total coefficient of thermal conductivity given by Hirschfelder[24] is just the sum of the inert and reactive parts:

$$\kappa = \kappa_{inert} + \kappa_{reactive} \tag{31}$$

The estimated coefficients of thermal conductivity are shown for pressures of 10^0, 10^{-2} and 10^{-4} atmospheres as a function of temperature in Figure 7. Again the ordinate is normalized by an inert gas value given by

$$\kappa_0 = \frac{19}{4}\frac{R}{M_0}\mu_0 \tag{32}$$

The thermal conductivity goes through pronounced maxima at temperatures where the chemical activity is intense. As shown in Figure 7, the coefficient may become one to two orders of magnitude larger than the inert gas value. The maxima occur at about the same temperature where the compressibility changes most rapidly with temperature (Fig. 2) and therefore where the specific heats are a maximum. In fact, Hirschfelder[24] has noted that the thermal conductivity should be approximately proportional to the specific heat for the chemically reacting gas just as it is for the inert gas (Eq. 27). It follows that the Prandtl number should not be grossly affected by the reactions, at least up to the temperature where the ionization reactions occur. The highly ionized gas is a mixture of very light-weight particles (electrons) with heavy particles (ions) and the effect of this mass difference is to increase greatly the ratio of thermal conductivity to viscosity. Thus, if the ionized gas is everywhere in thermal equilibrium, it should have a very small Prandtl number, of the order of 10^{-2} (see Ref. 9).

Some very approximate assumptions are used in the foregoing calculations of the transport properties, and it is obviously desirable to check them with experiment in some manner. It seems difficult to obtain the transport coefficients directly by experiment at the very high temperatures involved, but it has been possible to evaluate a quantity called the heat flux potential by combining some results of shock tube experiments with the theory of heat diffusion through gases. The heat flux potential is defined as

$$\phi = \int_0^T \kappa \, dT \tag{33}$$

so it represents a transport property. This integral has the quality of a potential, since the heat flux at any point in a medium is just grad ϕ. The heat flux potential is the natural parameter to use as the dependent variable in problems involving heat diffusion through media where the thermal conductivity is a function of temperature, as it is for gases. In terms of ϕ, the heat diffusion equation takes the familiar form

$$\frac{\partial \phi}{\partial t} - a \nabla^2 \phi = 0 \tag{34}$$

where a is the thermal diffusivity, $k/\rho C_p$. Note that the diffusivity cannot be considered a constant as is usually done in the classical solutions of the heat diffusion equation (see Ref. 27, for example).

Consider now the one-dimensional heat flow through a semi-infinite gas medium. We shall restrict ourselves to the case where the initial conditions and the boundary conditions are constants; that is, the initial potential throughout the gas is the constant designated by ϕ_∞, and the boundary value is the constant ϕ_0 (see Fig. 8). The diffusivities are a_∞ and a_0, respectively. Normalized coordinates will be used such that ϕ_0 and a_0 are both taken to be unity. The results can easily be generalized, of course, to account for arbitrary units of these boundary conditions.

The idealization of constant initial and boundary conditions will be approximately realized in a physical situation where the reservoir is a slab of material with a very large heat capacity and a large thermal conductivity, such as a metal. Then the wall can soak up heat fast enough to maintain nearly constant conditions at the interface. The slab might be suddenly immersed in a constant temperature gas, for example; or, alternatively, the gas might be heated suddenly by a plane shock wave reflecting from the solid interface.

Boltzmann[28] has shown, with perfect generality, that the solution to this problem may be expressed as a function of $x/\sqrt{t}$. Therefore, the time and distance variables are transformed to the single dimensionless parameter

$$y = \frac{x}{\sqrt{(4a_0 t)}} \tag{35}$$

where a_0 is the diffusivity of the gas at the boundary; a_0 is unity, of course, in the present normalized coordinate system, but this is not an essential feature of

the transformation. In terms of this parameter, y, the partial differential equation of heat conduction becomes the dimensionless, total differential equation

$$a \frac{d^2\phi}{dy^2} + 2y \frac{d\phi}{dy} = 0 \tag{36}$$

The factor 4 in the parameter y (Eq. 35) is an arbitrary stretching factor. It is chosen merely so that the solutions to Equation (36) reduce to the usual error function form when the diffusivity is constant, that is, when a equals a_0. The merit in using the normalized form for the potential ϕ (that is, ϕ/ϕ_0) is that one set of integrations for Equation (36) will suffice for all possible boundary conditions. All that is required before one proceeds with the integration is that the diffusivity, a, be evaluated. Two cases will be considered, one in which the gas is ideal and inert, and the second in which the gas is in local equilibrium but is chemically active with a large heat of reaction.

According to the kinetic theory of inert gases[13], the coefficient of thermal conductivity is approximately proportional to a power b of the temperature, where b is close to ½. Thus the integral of thermal conductivity is proportional to the $(b+1)^{th}$ power of temperature:

$$\phi = \int \kappa \, dT \propto T^{b+1} \tag{37}$$

Now the thermal diffusivity equals the conductivity divided by the heat capacity per unit volume, $C\rho$. Since the density ρ is inversely proportional to temperature, for an ideal gas, the diffusivity is proportional to the $(b+1)^{th}$ power of temperature also:

$$a = \frac{\kappa}{C\rho} \propto T^{b+1} \tag{38}$$

It follows that diffusivity is proportional to the potential ϕ, and in the present normalized coordinates this means that

$$a = \phi \tag{39}$$

Sometimes a linear relation between a and ϕ with a finite intercept will best fit measured values, but this can always be transformed to the direct proportionality of Equation (30) by appropriate adjustment of the lower limit of the integral, Equation (33). Generally, this limit will be close to absolute zero.

It may be remarked that even if one accounts for the variations of heat capacity which occur in a real gas, the preceding relations are valid to the order of approximation that Prandtl number is a constant. This can be seen from the fact that diffusivity is just the kinematic viscosity divided by the Prandtl number:

$$a = \frac{\mu/\rho}{Pr} \tag{40}$$

and the kinematic viscosity is again approximately proportional to the $(b+1)^{th}$ power of temperature, at least in gases composed of neutral particles.

When the result of Equation (39) is used, the heat diffusion equation takes on the inocuous looking form

$$\phi \frac{d^2\phi}{dy^2} + 2y \frac{d\phi}{dy} = 0 \tag{41}$$

Analytic solutions to Equation (41) are known, but none which satisfies the boundary conditions, namely:

$$\phi(0) = 1 \tag{42a}$$

$$\lim_{y \to \infty} \phi \to \phi_\infty \tag{42b}$$

This is somewhat frustrating in view of the deceptively simple appearance of the non-linear Equation (41). However, it is relatively easy to integrate the equation numerically, starting from a given value of the boundary derivative, $\phi_0' = (d\phi/dy)_0$, and terminating as the solution asymptotically approaches a limit, ϕ_∞. The solutions are something like error functions stretched slightly out of shape. Three of these solutions are shown in Figure 9 as a function of $y/\sqrt{\phi_\infty}$. The solutions ϕ are shown divided by the error functions $1 + (\phi_\infty - 1)\text{erf}\, y/\sqrt{\phi_\infty}$. The ϕ functions rise more steeply than the error functions near the orgin, go through a maximum deviation, then approach the error function as a limit.

The value of ϕ_∞ is uniquely related to the derivative at the origin, ϕ_0'. This relation is shown in Figure 10. The derivative ϕ_0' is equivalent to a dimensionless heat flux at the boundary, while the normalizing function, $1 + \sqrt{1/4\pi}\,\phi_0'$, is the value which ϕ_∞ would have if diffusivity were a constant. We shall return to this relation between ϕ_∞ and ϕ_0' after considering the case of the chemically reacting gas.

A chemical reaction in the gas behaves like a reservoir which soaks up heat as temperature is increased, and liberates heat when temperature drops. Consequently, the specific heat is very large if the heat of reaction is large compared to RT. Hirschfelder[24] has shown that the coefficient of thermal conductivity for gases in local equilibrium is also very large; in fact, it is approximately proportional to the specific heat. Thus, the Prandtl number is relatively constant and the diffusivity is a function of temperature which is not greatly affected by the chemical reaction. The integral of thermal conductivity, on the other hand, is greatly increased as a result of the reaction. This situation is illustrated in Figure 11.

The diffusivity increases linearly with ϕ up to the point where the chemical reaction occurs, there it flattens out until the reaction is about complete, then it increases again in a more or less linear manner. The solid lines are the previously discussed theoretical estimates for air in which oxygen dissociation occurs. The pressure dependence of the curve for ϕ less than $2\phi_c$ has been removed by normalizing both ordinate and abscissa with the factor ϕ_c:

$$\phi_c = \left(\frac{T_c}{T_0}\right)^{b+1} \tag{43}$$

where T_0 is the boundary temperature, and T_c is the temperature where the thermal conductivity is a maximum, that is, where the diffusivity is most nearly independent of the conductivity integral. The temperature T_c may be calculated from Equation (28).

It should be noted that the calculation of the relation between diffusivity and the conductivity integral does not depend on precise numerical values of the transport coefficients. For example, although the estimate shown for air in Figure 11 is based on simple kinetic theory and very approximate collision cross sections, the corrections introduced by more exact calculations affect both the diffusivity and the conductivity simultaneously in such a way that the functional relation between the two is maintained.

The relation for reacting gases in general will be similar to that for air. The dashed curve on Figure 11 is a limit which is approached as the heat of reaction becomes very large. This limiting relation has been used in the integrations which follow, that is, a is assumed to equal ϕ up to the point ϕ_c and thereafter is taken to be constant. Up to the point ϕ_c then, the solutions are the stretched-out error functions which were discussed earlier and which are shown in Figure 9. At ϕ_c, these solutions are joined by the solution for constant diffusivity which has a matching slope at the junction, $(d\phi/dy)_c$:

$$\phi = \phi_c + \sqrt{\frac{\pi\phi_c}{4}}\left(\frac{d\phi}{dy}\right)_c \left(\exp\frac{y^2}{\phi_c}\right)\left(\operatorname{erf}\frac{y}{\sqrt{\phi_c}} - \operatorname{erf}\frac{y_c}{\sqrt{\phi_c}}\right) \tag{44}$$

In Figure 12, the limit of the potential ϕ_∞ is shown for a reacting gas as a function of the boundary heat flux, ϕ_0'. The solution now depends on the value of ϕ_c, which in turn depends on the boundary temperature, the pressure, and the chemical reaction being considered. For example, in the case of air and a boundary temperature of 0^0 C, the values 20, 40 and 60 for ϕ_c correspond to pressures of about 10^{-4}, 10^0 and 10^2 atmospheres, respectively. The solutions for values of ϕ_c corresponding to other pressures and different boundary temperatures can be obtained fairly accurately by interpolation between the numerically integrated solutions such as the curves plotted in Figure 12. The inert gas solution (Fig. 10) corresponds to ϕ_c equal to infinity (Fig. 12). It should be noted that these solutions can only be used up to the point where the chemical reaction goes to completion. Beyond this, the increase in diffusivity must again be taken into account. The domain of validity is a characteristic of each specific reaction. Within this limitation, the curves of Figure 12 apply to chemically reacting gases in general.

The above solutions have been put to use, in conjunction with experiment, to evaluate the heat flux potential as a function of temperature[29,30]. In this experiment, a plane shock wave is reflected from the end wall of a shock tube. The heat flux to the wall is measured, and this fixes the abscissa for the graphical solution on Figure 12. The temperature at the wall and the pressure of the gas after the shock reflection determine the value of ϕ_c (see Eq. 43). Hence the value of the ordinate in Figure 12 is fixed, and the value of ϕ_∞ is determined. The temperature of the gas associated with this heat flux potential ϕ_∞ is taken to be the equilibrium temperature after the shock reflection, and this is a known function of the measured shock velocity. This procedure, of course, implies that the experiments are conducted under conditions where the chemical relaxation times are short compared to the test interval.

Results of the experiments and calculations are shown in Figure 13. The heat flux potential is shown divided by the inert gas value, where the coefficient b is taken to be 1/2

$$\phi_{inert} = \frac{2}{3} \kappa_0 T_0 \left(\frac{T}{T_0}\right)^{3/2} \simeq 3.2 \times 10^{-6} T^{3/2} \quad \frac{cal}{cm\ sec} \tag{45}$$

and where T is in degrees Kelvin. Thus the ratio ϕ/ϕ_{inert} should be unity if the coefficient of thermal conductivity is proportional to the 1/2-power of temperature. This appears to be approximately true up to the temperature where oxygen dissociation begins. At the pressures involved in the present shock tube experiments, this occurred at about 2500°K. At higher temperatures, the heat flux potential becomes more than twice as large as the inert gas value as a result of the dissociation of oxygen. The solid curve on Figure 13 shows the theoretical heat flux potential, based on the estimates for the coefficients of thermal conductivity. The agreement between the experiment and theory is about as good as the scatter in the data and is somewhat better than the uncertainty expected of the theory. The small deviation from inert gas behavior which occurs just before the dissociation reaction has been explained[30] as the result of small increases in the thermal conductivity integral due to vibrational energy excitation and to formation and ionization of nitric oxide. The theory and experiment appear to agree on the large change due to oxygen dissociation, and it is believed that the theoretical estimates may represent a reasonable approximation to use for some engineering purposes. However, it is clear that the experimental results give merely a necessary but not sufficient check on the validity of the approximate methods used to evaluate the transport coefficients. It may be noted that the potential shown in Figure 13 is not a constant pressure function but follows the particular progression of pressures obtained with the various strength shock waves produced for the experiment. The theoretical potentials are shown in Figure 14 for temperatures up to 8000°K and for constant pressures from 10^2 to 10^{-4} atmospheres. Interpolations can be made approximately in proportion to the logarithm of pressure.

4. CONCLUDING REMARKS

To summarize, some methods have been outlined by which thermodynamic properties of air can be approximated in closed form with an accuracy generally somewhat better than 5% for temperatures up to 15,000°K and for pressures from 10^{-6} to 10^2 atmospheres. The solutions are analytic in terms of temperature and pressure or of temperature and density as the independent variables. A single series of iterations suffices for calculation of constant entropy properties.

The equilibrium mol fractions have been used for estimates of the viscosity and thermal conductivity for air. These estimates are based on the elementary kinetic theory of colliding elastic spheres where the size of the sphere is allowed to vary with temperature so as to account for some functional dependence of collision cross section on velocity. The coefficient of thermal conductivity integrated with respect to temperature is a heat flux potential and is found to be the natural parameter to use as the dependent variable in problems involving heat diffusion through gases. This potential has been evaluated by experiment for air up to 5000°K, including the effect of oxygen dissociation, and the results are found to agree reasonably well with the theoretical estimates.

REFERENCES

1. Gilmore, F.R. — *Equilibrium Composition and Thermodynamic Properties of Air to 24,000° K.* Rand Rep. RM-1543, Aug. 24, 1955.

2. Hilsenrath, Joseph; Beckett, Charles W. — *Tables of Thermodynamic Properties of Argon-Free Air to 15,000° K.* Arnold Engr. Dev. Center, TN-56-12, Sept. 1956.

3. Logan, J.G., Jr.; Treanor, C.E. — *Tables of Thermodynamic Properties of Air From 3000° K to 10,000° K at Intervals of 100° K.* Cornell Aero. Lab. Rep. BE-1007-A-3, Jan. 1957.

4. Feldman, Saul. — *Hypersonic Gas Dynamic Charts for Equilibrium Air.* AVCO Res. Lab., Jan. 1957.

5. Moeckel, W.E.; Weston, Kenneth C. — *Composition and Thermodynamic Properties of Air in Chemical Equilibrium.* NACA TN 4265, 1958.

6. Romig, Mary F. — *The Normal Shock Properties for Air in Dissociation Equilibrium.* Jour. Aero. Sci., vol. 23, no. 2, Feb. 1956, p.185.

7. Hochstim, Adolf R. — *Gas Properties Behind Shocks at Hypersonic Velocities. I. Normal Shocks in Air.* Rep. No. ZPh(GP)-002, Convair, Jan. 30, 1957.

8. Hansen, C. Frederick; Heims, Steve P. — *A Review of the Thermodynamic, Transport and Chemical Reaction Rate Properties of High-Temperature Air.* NACA TN 4359, 1958.

9. Hansen, C. Frederick. — *Approximations for the Thermodynamic and Transport Properties of High-Temperature Air.* NASA TR-50, 1959.

10. Courant, R.; Friedrichs, K.O. — *Supersonic Flow and Shock Waves.* Interscience Publishers, Inc., 1948.

11. Hansen, C. Frederick.; Hodge, Marion E. — *Constant Entropy Properties for an Approximate Model of Equilibrium Air.* NASA TN D-352, 1960.

12. Chapman, S.; Cowling, T.G. — *The Mathematical Theory of Non-Uniform Gases.* Cambridge Univ. Press, 1939.

13. Kennard, E.H. — *Kinetic Theory of Gases.* McGraw Hill Book Co., 1938.

14. Vanderslice, Joseph T. et alii — *Interactions Between Ground State Nitrogen Atoms and Molecules.* NASA MEMO 4-13-59W, 1959.

15. Vanderslice, Joseph T. et alii — *Interaction Between Oxygen and Nitrogen O-N, O-N_2, and O_2-N_2*.* University of Maryland, Institute of Molecular Physics, Rep. IMP-NASA-8, Feb. 1959.

16. Hammerling, P. et alii — *Low Energy Elastic Scattering of Electrons by Oxygen and Nitrogen.* Jour. Appl. Phys., vol. 28, no. 7, 1957, pp. 760-764. (AVCO Res. Rep. 6, 1957).

17. Meador, Willard E., Jr. — *The Interactions Between Nitrogen and Oxygen Molecules.* NASA TR R-68, 1960.

18. Hirschfelder, J.O. Eliason, M.O. — *The Estimation of the Transport Properties for Electronically Excited Atoms and Molecules.* Univ. Wisconsin Tech. Rep. WIS-AF-1, May 1956.

19. Herzberg, Gerhard. — *Molecular Spectra and Molecular Structure. I. Spectra of Diatomic Molecules.* Second ed., D. Van Nostrand Co., Inc., 1950.

20. Cohen, Robert S. et alii — *The Electrical Conductivity of an Ionized Gas.* Phys. Rev., vol. 80, no. 2, Oct. 1950, pp. 230-238.

21. Hirschfelder, J.O. et alii — *Molecular Theory of Gases and Liquids.* J. Wiley and Sons, 1954.

22. Buddenberg, J.W. Wilke, C.R. — *Calculation of Gas Mixture Viscosities.* Industrial and Engineering Chemistry, vol. 41, July 1949, pp. 1345-1347.

23. Nernst, W. — *Chemisches Gleichgewicht und Temperaturgefalle.* Ludwig Boltzmann Festschrift, verlag von J. A. Barth, Leipzig, 1904, pp. 904-915.

24. Hirschfelder, Joseph O. — *Heat Transfer in Chemically Reacting Mixtures.* I. Jour. Chem. Phys., vol. 26, no. 2, Feb. 1957, pp. 274-281.

25. Eucken, A. — *Über das Wärmeleitvermögen, die spezifische Wärme und die innere Reibung der Gase.* Physikalische Zeitschrift, Vol. 14, no. 8, Apr. 1913, pp. 324-332.

26. Butler, James N. Brokaw, Richard S. — *Thermal Conductivity of Gas Mixtures in Chemical Equilibrium.* Jour. Chem. Phys., vol. 26, no. 6, June 1957, pp. 1636-1643.

27. Carslaw, H.S. Jaeger, J.C. — *Conduction of Heat in Solids.* Oxford Press, 1947.

28. Boltzmann, Ludwig. — *Zur Integration der Diffusionsgleichung bei Variabeln Diffusionscoefficienten.* Annalen der Physik, vol. 53, 1894, pp. 959-964.

29. Hansen, C. Frederick. et alii — *Theoretical and Experimental Investigation of Heat Conduction in Air, Including Effects of Oxygen Dissociation.* NASA Rep. 27, 1959.

30. Peng, Tzy-Cheng Ahtye, Warren F. — *Experimental and Theoretical Study of Heat Conduction for Air up to 5000° K.* NASA TN D-687, 1960.

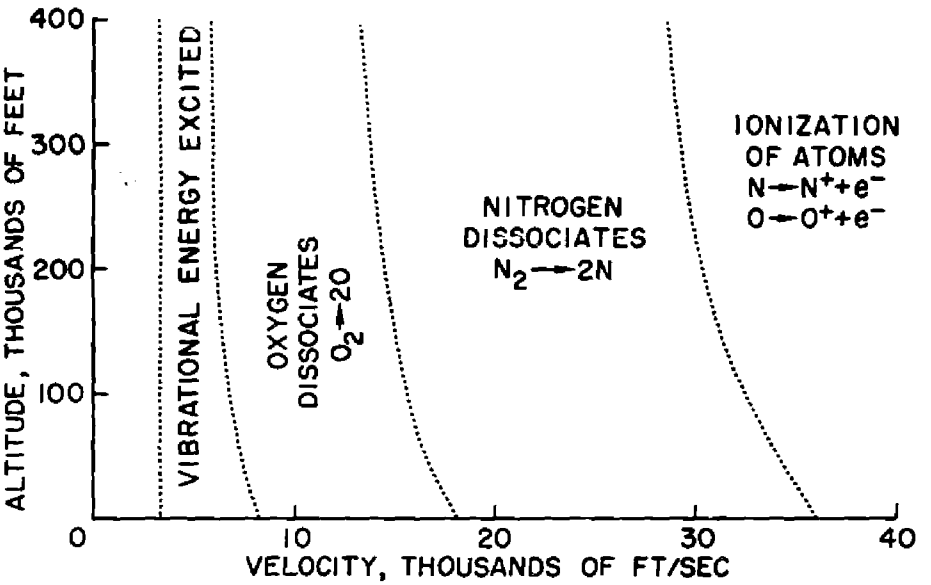

Fig.1 Stagnation region chemistry

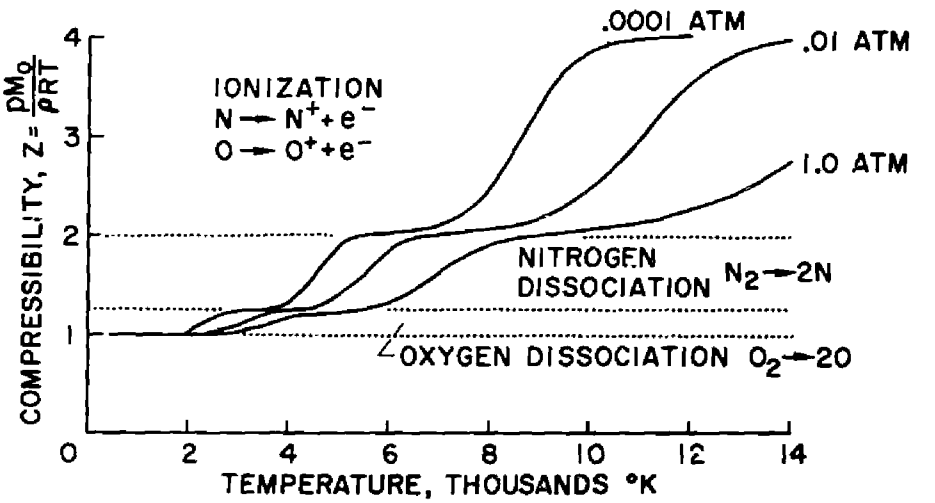

Fig.2 Compressibility for air in equilibrium

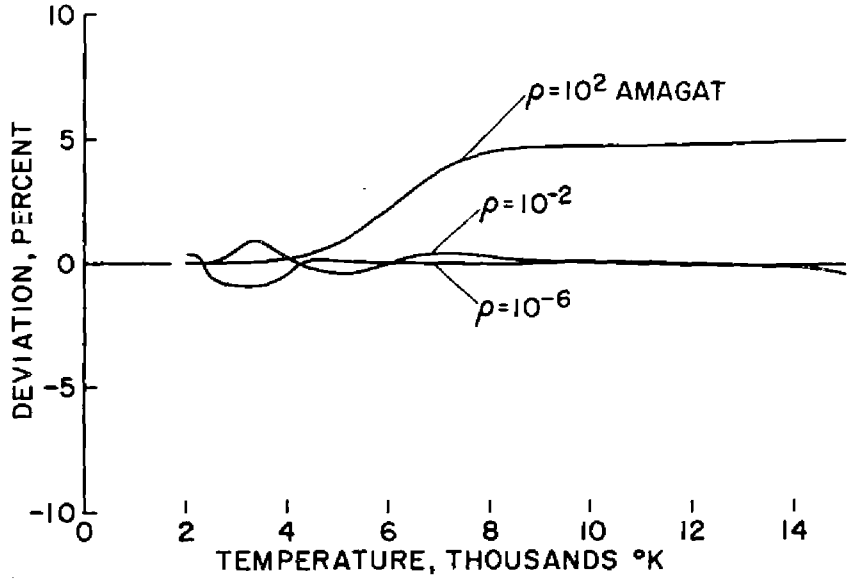

(a) Deviations in compressibility

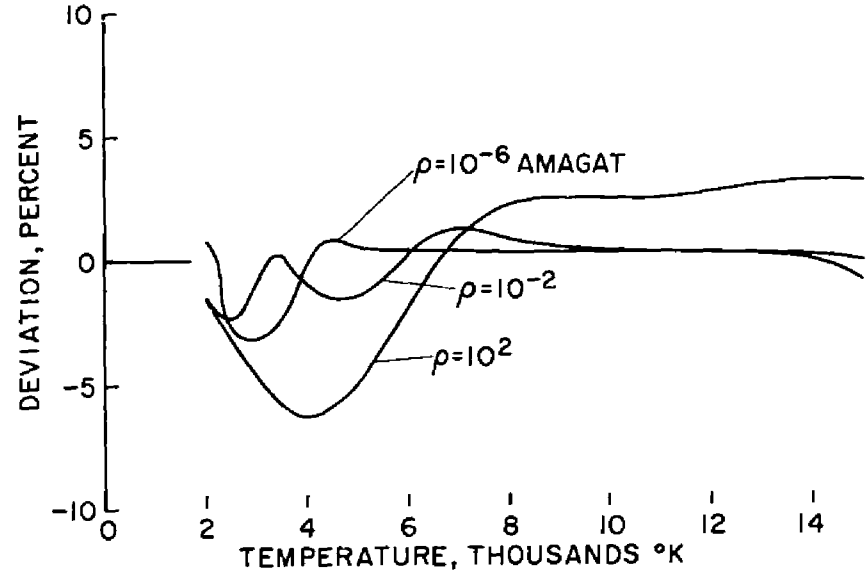

(b) Deviations in enthalpy

Fig.3 Deviations in the approximate solutions for thermodynamic properties of air

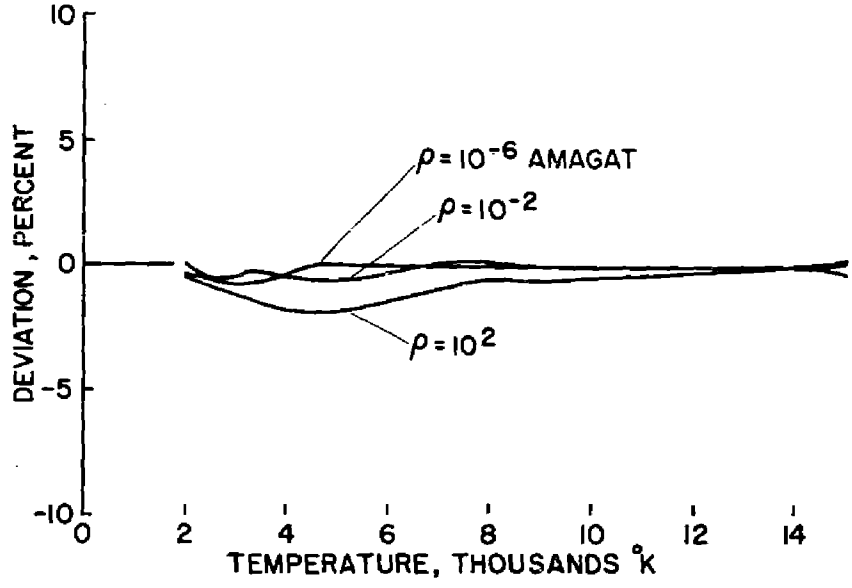

(c) Deviations in entropy

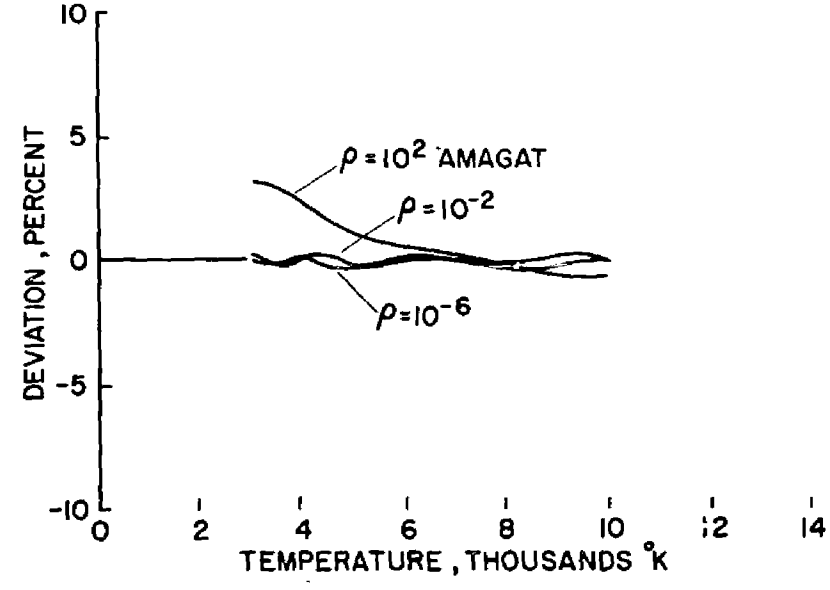

(d) Deviations in ratio of specific heats

Fig.3 Concluded

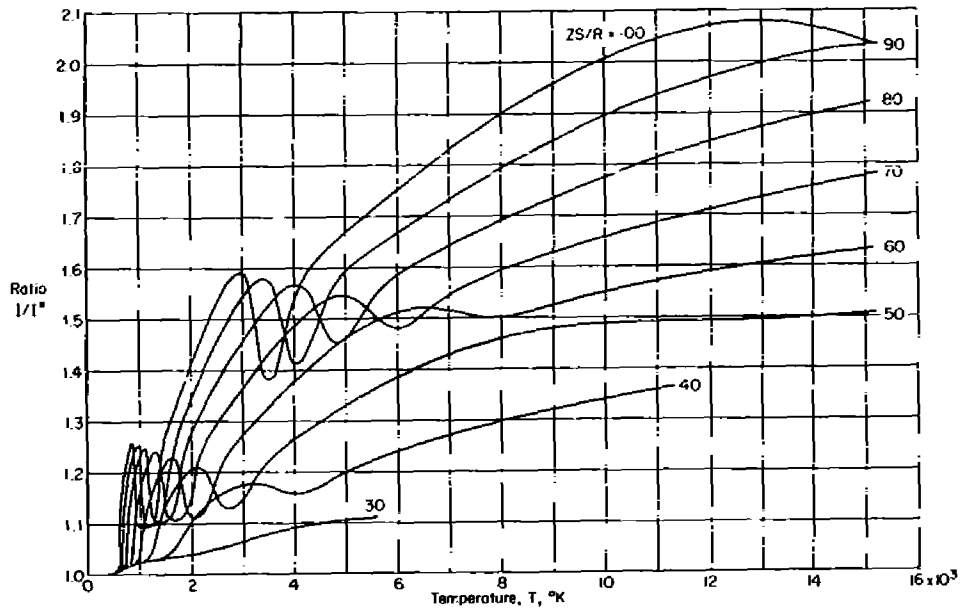

Fig.4 Ratio I/I^* as a function of temperature for constant entropy

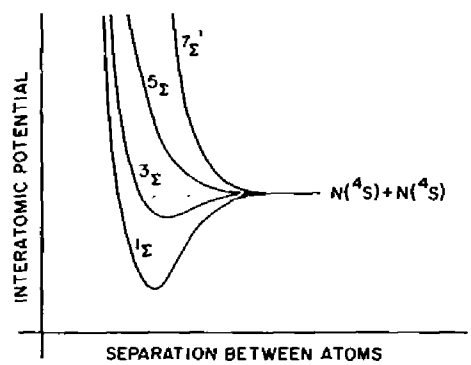

Fig.5 Schematic potentials between nitrogen atoms

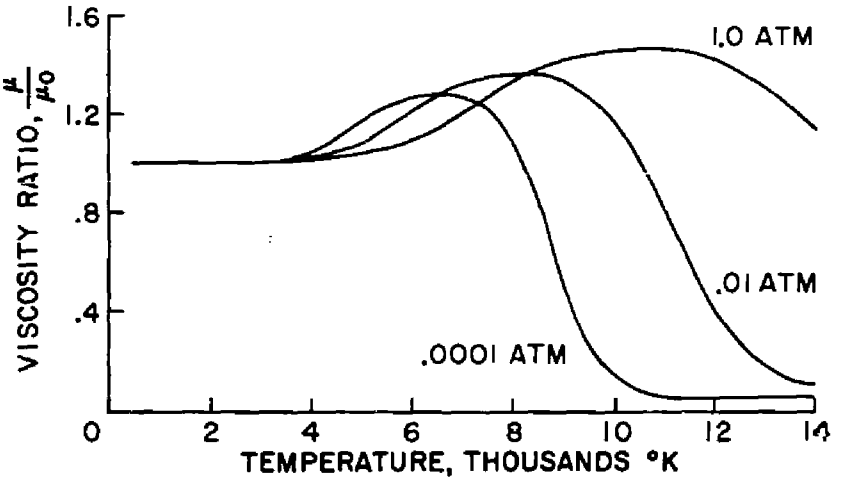

Fig. 6 Viscosity for air

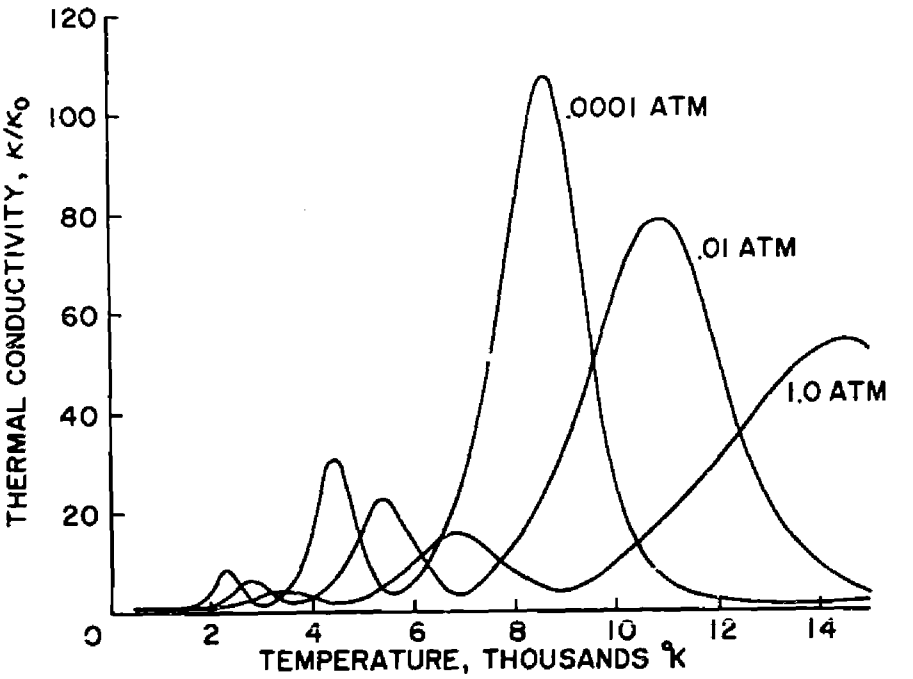

Fig. 7 Thermal conductivity for air

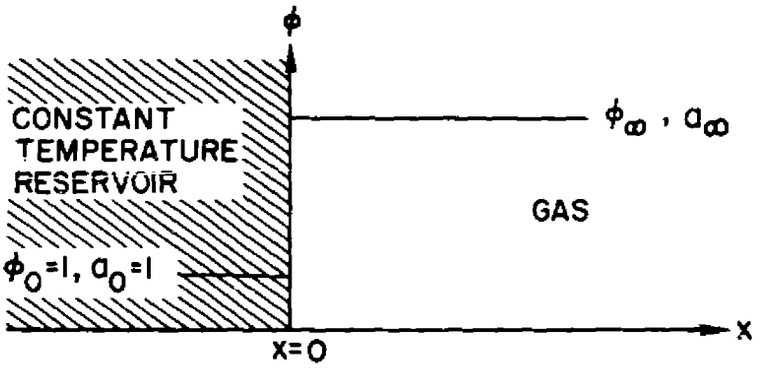

Fig. 8 One-dimensional heat diffusion

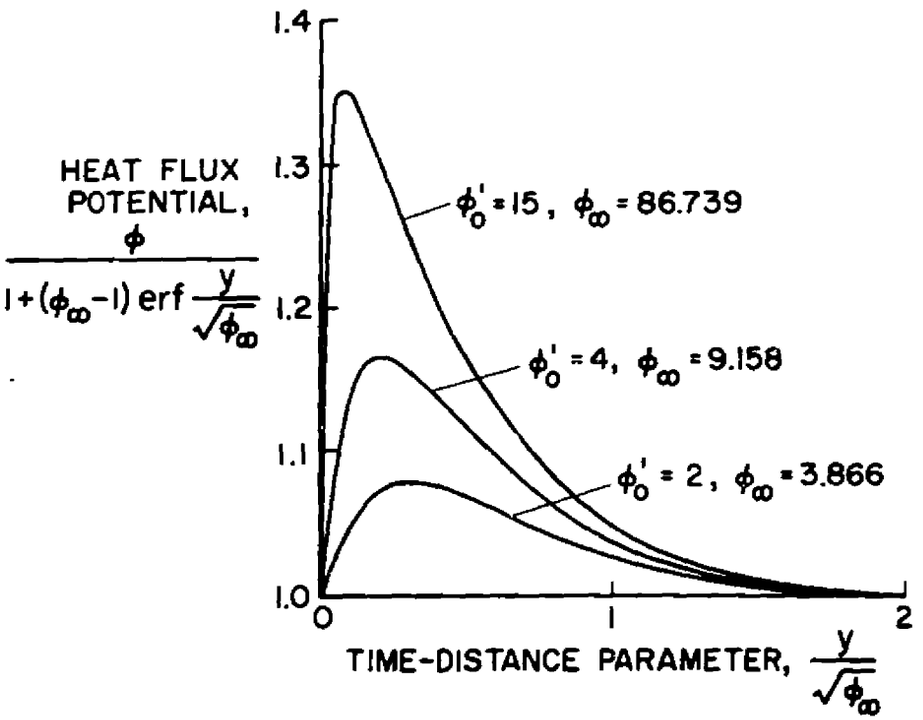

Fig. 9 Solutions for heat diffusion in inert gases

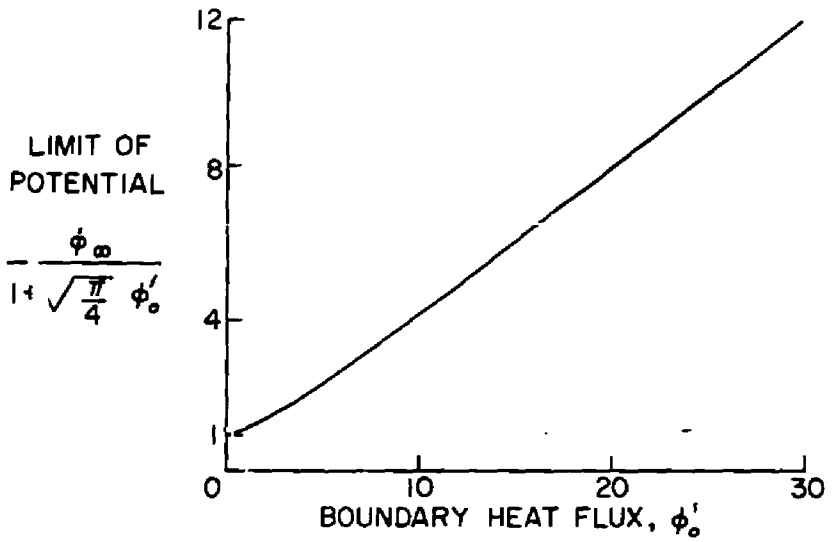

Fig.10 Heat diffusion in inert gases

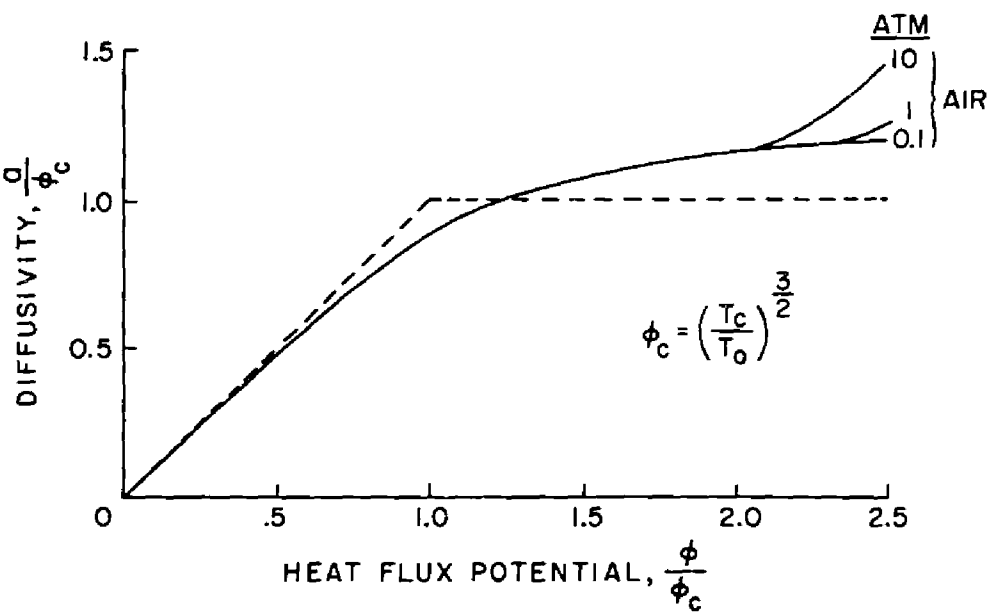

Fig.11 Diffusivity function

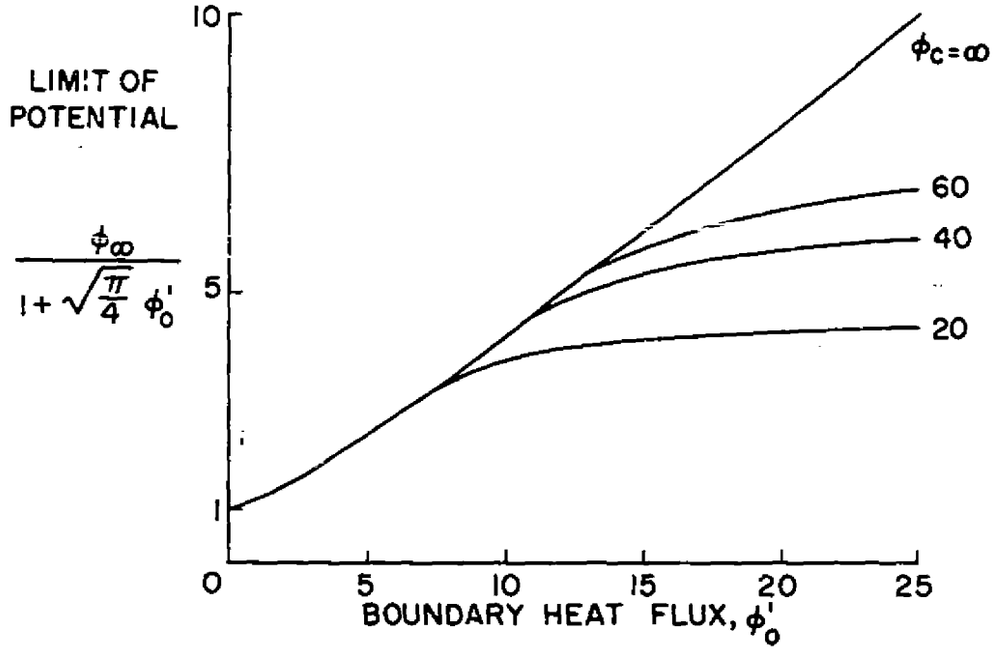

Fig. 12 Chemical equilibrium heat diffusion

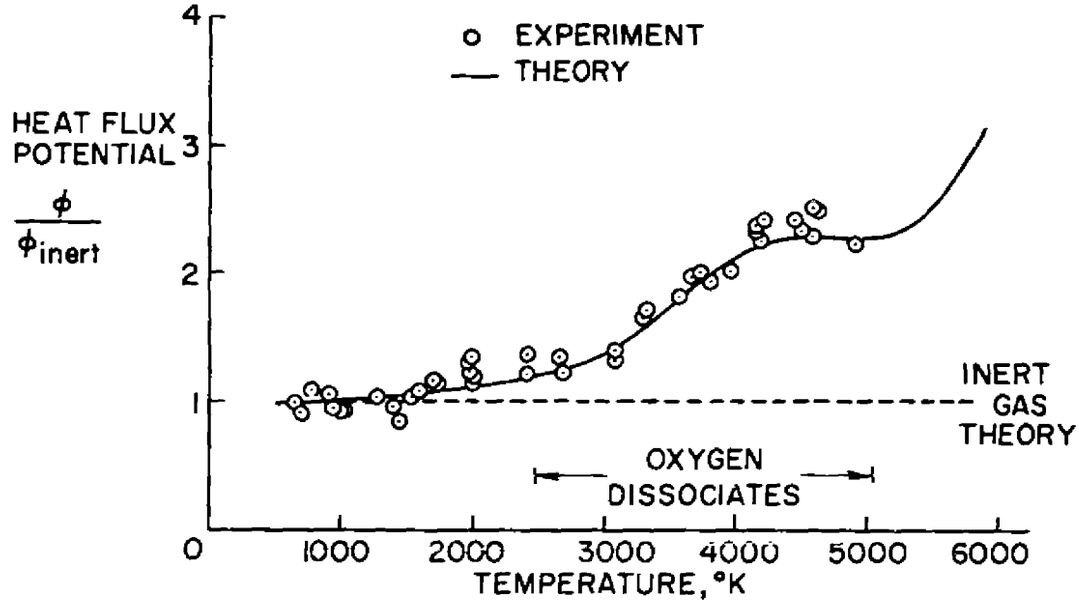

Fig. 13 Experimental heat flux potential for air

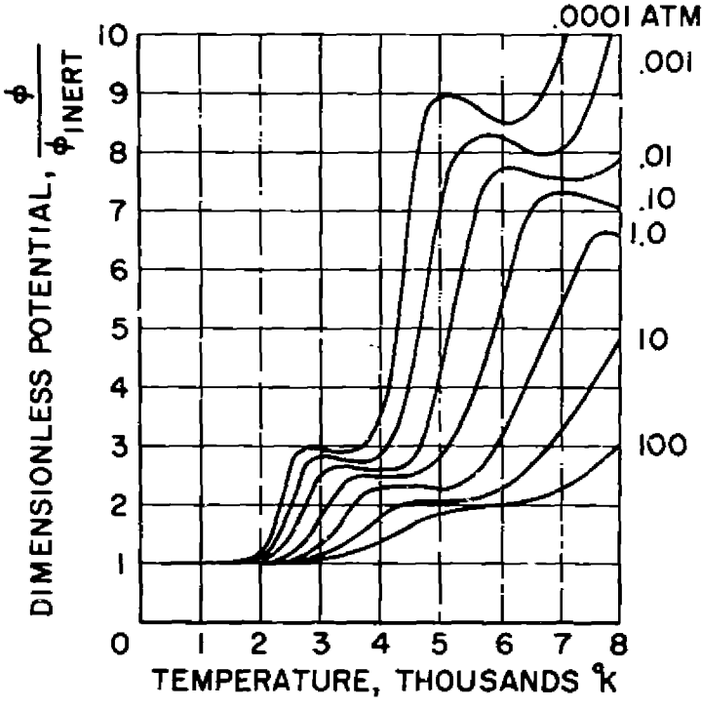

Fig.14 Theoretical heat flux potential for air

DISTRIBUTION

Copies of AGARD publications may be obtained in the various countries at the addresses given below.

On peut se procurer des exemplaires des publications de l'AGARD aux adresses suivantes.

BELGIUM BELGIQUE	Centre National d'Etudes et de Recherches Aéronautiques 11, rue d'Egmont, Bruxelles
CANADA	Director of Scientific Information Service Defense Research Board Department of National Defense 'A' Building, Ottawa, Ontario
DENMARK DANEMARK	Military Research Board Defense Staff Kastellet, Copenhagen Ø
FRANCE	O.N.E.R.A. (Direction) 25, Avenue de la Division Leclerc Châtillon-sous-Bagneux (Seine)
GERMANY ALLEMAGNE	Wissenschaftliche Gesellschaft für Luftfahrt Zentralstelle der Luftfahrtdokumentation Munchen 64, Flughafen Attn: Dr. H.J. Rautenberg
GREECE GRECE	Greek National Defense General Staff B. MEO Athens
ICELAND ISLANDE	Director of Aviation c/o Flugrad Reykjavik
ITALY ITALIE	Ufficio del Generale Ispettore del Genio Aeronautico Ministero Difesa Aeronautica Roma
LUXEMBURG LUXEMBOURG	Obtainable through Belgium
NETHERLANDS PAYS BAS	Netherlands Delegation to AGARD Michiel de Ruyterweg 10 Delft

NORWAY NORVEGE	Mr. O. Blichner Norwegian Defence Research Establishment Kjeller per Lilleström
PORTUGAL	Col. J.A. de Almeida Viama (Delegado Nacional do 'AGARD') Direcção do Serviço de Material da F.A. Rua da Escola Politecnica, 42 Lisboa
TURKEY TURQUIE	Ministry of National Defence Ankara Attn. AGARD National Delegate
UNITED KINGDOM ROYAUME UNI	Ministry of Aviation T.I.L., Room 009A First Avenue House High Holborn London W.C.1
UNITED STATES ETATS UNIS	National Aeronautics and Space Administration (NASA) 1520 H Street, N.W. Washington 25, D.C.

Printed by Technical Editing and Reproduction Ltd
95 Great Portland St. London, W.1.

AGARD Report 323 North Atlantic Treaty Organization, Advisory Group for Aeronautical Research and Development THERMODYNAMIC AND TRANSPORT PROPERTIES OF HIGH-TEMPERATURE AIR C. Frederick Hansen 1959 26 pages, incl. 30 refs., 14 figs. It is well known that vehicles traveling at high speed excite the air to high temperature, resulting in dissociation and ionization, so that the air properties deviate considerably from those of a simple gas. Some effects of these reactions are considered in this Report in relation to the thermodynamic properties of the air, the transport coefficients, and the diffusion of heat. P.T.O.	536.7 1c3b:3b1e	AGARD Report 323 North Atlantic Treaty Organization, Advisory Group for Aeronautical Research and Development THERMODYNAMIC AND TRANSPORT PROPERTIES OF HIGH-TEMPERATURE AIR C. Frederick Hansen 1959 26 pages, incl. 30 refs., 14 figs. It is well known that vehicles traveling at high speed excite the air to high temperature, resulting in dissociation and ionization, so that the air properties deviate considerably from those of a simple gas. Some effects of these reactions are considered in this Report in relation to the thermodynamic properties of the air, the transport coefficients, and the diffusion of heat. P.T.O.	536.7 1c3b:3b1e
AGARD Report 323 North Atlantic Treaty Organization, Advisory Group for Aeronautical Research and Development THERMODYNAMIC AND TRANSPORT PROPERTIES OF HIGH-TEMPERATURE AIR C. Frederick Hansen 1959 26 pages, incl. 30 refs., 14 figs. It is well known that vehicles traveling at high speed excite the air to high temperature, resulting in dissociation and ionization, so that the air properties deviate considerably from those of a simple gas. Some effects of these reactions are considered in this Report in relation to the thermodynamic properties of the air, the transport coefficients, and the diffusion of heat. P.T.O.	536.7 1c3b:3b1e	AGARD Report 323 North Atlantic Treaty Organization, Advisory Group for Aeronautical Research and Development THERMODYNAMIC AND TRANSPORT PROPERTIES OF HIGH-TEMPERATURE AIR C. Frederick Hansen 1959 26 pages, incl. 30 refs., 14 figs. It is well known that vehicles traveling at high speed excite the air to high temperature, resulting in dissociation and ionization, so that the air properties deviate considerably from those of a simple gas. Some effects of these reactions are considered in this Report in relation to the thermodynamic properties of the air, the transport coefficients, and the diffusion of heat. P.T.O.	536.7 1c3b:3b1e

Methods are presented for calculating the thermodynamic properties of air with good accuracy up to 15,000°K and for pressures from 10^{-6} to 10^{2} atmospheres.

This Report is one in the series 320-333 of papers presented at the High Temperature Gas Characteristics Meeting of the AGARD Wind Tunnel and Model Testing Panel (now Fluid Dynamics Panel) held 21-23 September 1959, in Aachen, Germany.

Methods are presented for calculating the thermodynamic properties of air with good accuracy up to 15,000°K and for pressures from 10^{-6} to 10^{2} atmospheres.

This Report is one in the series 320-333 of papers presented at the High Temperature Gas Characteristics Meeting of the AGARD Wind Tunnel and Model Testing Panel (now Fluid Dynamics Panel) held 21-23 September 1959, in Aachen, Germany.

Methods are presented for calculating the thermodynamic properties of air with good accuracy up to 15,000°K and for pressures from 10^{-6} to 10^{2} atmospheres.

This Report is one in the series 320-333 of papers presented at the High Temperature Gas Characteristics Meeting of the AGARD Wind Tunnel and Model Testing Panel (now Fluid Dynamics Panel) held 21-23 September 1959, in Aachen, Germany.

Methods are presented for calculating the thermodynamic properties of air with good accuracy up to 15,000°K and for pressures from 10^{-6} to 10^{2} atmospheres.

This Report is one in the series 320-333 of papers presented at the High Temperature Gas Characteristics Meeting of the AGARD Wind Tunnel and Model Testing Panel (now Fluid Dynamics Panel) held 21-23 September 1959, in Aachen, Germany.